Drug Delivery

DOI: 10.1002/ange.201407143

A Cancer-Targeted Nanosystem for Delivery of Gold(III) Complexes: Enhanced Selectivity and Apoptosis-Inducing Efficacy of a Gold(III) Porphyrin Complex**

Lizhen He, Tianfeng Chen, Yuanyuan You, Hao Hu, Wenjie Zheng, Wai-Lun Kwong, Taotao Zou, and Chi-Ming Che**

Abstract: *Construction of delivery systems for anticancer gold complexes to decrease their toxicity while maintaining efficacy is a key strategy to optimize and develop anticancer gold medicines. Herein, we describe cancer-targeted mesoporous silica nanoparticles (MSN) for delivery of a gold(III) porphyrin complex (Au-1a@MSN(R)) to enhance its anticancer efficacy and selectivity between cancer and normal cells. Encapsulation of Au-1a within mesoporous silica nanoparticles amplifies its inhibitory effects on thioredoxin reductase (TrxR), resulting in a loss of redox balance and overproduction of reactive oxygen species (ROS). Elevated cellular oxidative stress activates diversified downstream ROS-mediated signaling pathways, leading to enhanced apoptosis-inducing efficacy.*

The limitations of cisplatin-based chemotherapy has prompted intense interest among scientists to search for alternative metal-based anticancer medicines.[1] Among the non-platinum antitumor agents, gold complexes are receiving increasing attention because of their promising in vitro and in vivo anticancer activities.[2,3] Activation of mitochondrial dysfunctions and other apoptotic cellular events, and interaction with some specific enzymatic targets, such as selenol- or thiol-containing thioredoxin reductase (TrxR), glutathione reductase, and peroxidase, have been proposed to account for the anticancer activities of gold complexes.[4] TrxR has been proposed to be a potential cellular target of gold complexes, as a result of the high affinity of gold ions towards the cysteine and selenocysteine residues at the active site of TrxR.[5] We have demonstrated that gold(III) porphyrin complexes, as exemplified herein by $[Au^{III}(TPP)]Cl$ (Au-1a; H_2TPP = 5,10,15,20-tetraphenylporphyrin; Figure 1a), exhibited novel anticancer activity which is substantially higher than cisplatin, and could target the mitochondria of cancer cells to activate intrinsic cell apoptosis with involvement of TrxR inhibition.[6] Nevertheless, further clinical application of Au-1a is hindered by its toxicity against normal cells and low solubility under physiological conditions. In fact, most anticancer gold complexes usually suffer similar shortcomings and some are not stable under physiological conditions.[7]

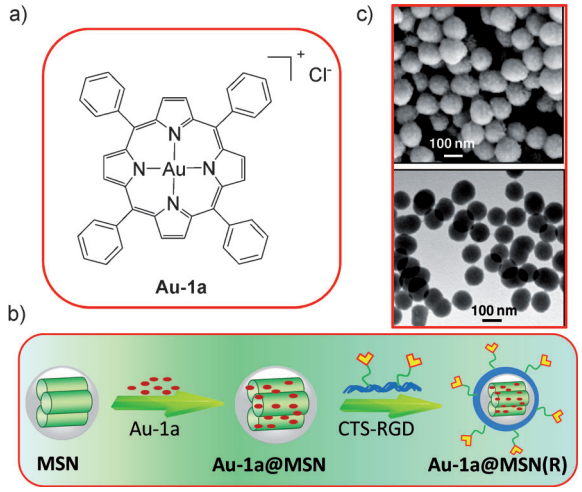

Figure 1. a) Chemical structure of Au-1a. b) The preparation of Au-1a-loaded microporous silica nanoparticles Au-1a@MSN(R). RGD is denoted by the yellow triangle. c) SEM and TEM images showing Au-1a@MSN(R) nanoparticles. Scale bars = 100 nm.

Nanotechnology-based delivery systems have been used in targeted therapy.[8] The enhanced permeability and retention (EPR) effect of nanoparticles endow them with the properties of easy internalization and excellent biodistribution in tumors, resulting in enhanced anticancer efficacy.[8,9] In this regard, mesoporous silica nanoparticles (MSN) have attracted attention as promising drug-delivery systems owing to their easy surface modification, high drug loading, and low-toxicity degradation pathways in biological environments.[10] For instance, Fang et al. synthesized dual-pore mesoporous carbon@silica composite core–shell nanospheres as a multi-

[*] L. He, Prof. Dr. T. F. Chen, Y. You, H. Hu, Dr. W. J. Zheng
Department of Chemistry, Jinan University
Guangzhou 510632 (China)
E-mail: tchentf@jnu.edu.cn
Dr. W.-L. Kwong, T. Zou, Prof. Dr. C.-M. Che
State Key Laboratory of Synthetic Chemistry
Institute of Molecular Functional Materials
Chemical Biology Center and Department of Chemistry
The University of Hong Kong, Pokfulam Road, Hong Kong (China)
E-mail: cmche@hku.hk
Prof. Dr. C.-M. Che
HKU Shenzhen Institute of Research and Innovation
Shenzhen 518053 (China)

[**] This work was supported by National High Technology Research and Development Program of China (2014AA020538), the National Key Basic Research Program of China (2013CB834802), Science Foundation for Distinguished Young Scholars of Guangdong Province, Natural Science Foundation of China, the University Grants Committee of Hong Kong SAR, China (Project no. AoE/P-03/08) and Special Equipment Grant of UGC (SEG_HKU02).
Supporting information for this article is available on the WWW under http://dx.doi.org/10.1002/anie.201407143.

drug delivery system for the treatment of human ovarian cancer.[11] Despite these positive results, studies also revealed the undesirable side effect of hemolysis of red blood cells during circulation, which were correlated with the interaction of the surface silanols of unmodified MSNs with endothelial and other normal cell membranes.[12] Coating the MSNs with a hydrophilic polymer shell can significantly decrease this toxicity and provide colloidal stability during blood circulation,[13] and could endow MSN with stimuli-responsive drug-release capabilities. Chitosan (CTS) is a biocompatible and biodegradable polymer.[14] The amino groups on the chains of CTS facilitates conjugation with various tumor-targeting molecules, such as folic acid, transferrin, the cell-penetrating TAT (transactivator of transcription) peptide, and RGD (arginylglycylaspartic acid). Chen et al. reported that functionalized microporous silica nanosystems could significantly enhance the anticancer efficacy of ruthenium polypyridyl complexes and decrease their toxicity towards normal human cells.[15] Herein, we described a cancer-targeted nanoscale drug-delivery system based on an RGD peptide-conjugated MSN as the carrier of a gold(III) porphyrin complex Au-1 a@MSN(R), where MSN(R) refers to MSN that was modified with RGD-CTS (Figure 1 b). The compound Au-1 a has been demonstrated to display potent in vivo anticancer activities towards drug-resistant cancers.[16] Au-1 a@MSN(R) accumulates and localizes in cancer cells, facilitating selective induction of apoptosis in cancer cells.

Au-1 a@MSN and Au-1 a@MSN(R) nanoparticles were prepared and characterized by various physical and chemical methods (details provided in the Supporting Information). The average particle size of the MSNs was approximately 102 nm, as measured using Zetasizer Nano-ZS particle analyzer (see Figure S1 in the Supporting Information). After loading with Au-1 a, the size of Au-1 a@MSN increased to 589 nm, which is attributed to the aggregation of the nanoparticles, as confirmed by a TEM image (Figure S2). Interestingly, after conjugation of CTS-RGD to the surface of the nanoparticles, the size of Au-1 a@MSN(R) decreased to 125 nm. The results of SEM, TEM, and high-resolution TEM images showed that Au-1 a@MSN(R) nanoparticles were highly monodisperse with diameters of approximately 100 nm (Figure 1 c and Figure S3). The zeta potential of Au-1 a@MSN was −17.9 mV, which increased to 19.4 mV after surface modification with CTS-RGD (Figure S4). It is possible that the presence of amino groups on the CTS moiety endowed Au-1 a@MSN(R) with positive charge, enhancing the stability and cellular uptake of Au-1 a@MSN(R). Au-1 a@MSN(R) displayed a similar UV/Vis absorption spectrum as Au-1 a, indicating the successful loading of Au-1 a into the pores of the MSN (Figure S5). Based on the results of the N_2 adsorption–desorption isotherm (Figure S6), the inflection point at the adsorption branches of the isotherm of Au-1 a@MSN(R) moved in the direction of low relative pressure, indicating the quantity of nitrogen capillary condensation declined after loaded with Au-1 a. The XPS spectra (XPS = X-ray photoelectron spectroscopy) also revealed the presence of gold within the Au-1 a@MSN(R) nanoparticles (Figure S7), consistent with the results of EDX analysis (EDX = energy-dispersive X-ray spectroscopy; Figure S8). The loading capacity and the efficiency of loading of Au-1 a were found to be 150.8 $\mu g\,mg^{-1}$ MSN and 15.1 %, respectively. The drug-release behavior of Au-1 a from the nanosystem was investigated in PBS solution (pH 7.4) and in A549 cell lysate to simulate the blood and intracellular environments, respectively. No significant drug release was detected in PBS (phosphate-buffered saline; pH 7.4), suggesting that Au-1 a@MSN(R) particles were stable during blood circulation (Figure S9). Under intracellular conditions, Au-1 a was released from the nanosystem in a time-dependent manner, revealing that the Au-1 a@MSN(R) nanoparticles were bio-responsive.

Au-1 a@MSN nanoparticles exhibited a higher anticancer activity than Au-1 a, but the toxicity towards L02 normal human cells was higher than that toward cancer cells (Figure S10). Therefore, RGD peptide was conjugated to MSNs by using CTS as a linker to improve the selectivity of the material between cancerous and normal cells. As shown in Figure 2 a, Au-1 a@MSN(R) exhibited higher anticancer activity against various human-cancer cell lines than the complex Au-1 a. In particular, A549 lung carcinoma cells displayed the highest sensitivity to Au-1 a@MSN(R) with an $IC_{50} = 0.18\ \mu M$, whereas the IC_{50} value for free Au-1 a was 1.13 μM. The nanosystem did not significantly increase the toxicity of Au-1 a against L02 human normal cells, whereas the drug carrier MSN alone was nontoxic toward the cancer and normal cells.[15] The safety index (the ratio of IC_{50} values of L02 cells to that for A549 cells) of Au-1 a@MSN(R) was found to be 4.23, which was significantly higher than those of Au-1 a (0.80) and Au-1 a@MSN (0.73).

Cellular uptake is an important factor contributing to anticancer activity. Therefore, quantitative analysis of cellular uptake of Au-1 a@MSN(R) in A549 lung carcinoma cells and L02 human normal liver cells were conducted by directly determining intracellular gold content with inductively coupled plasma mass spectrometry (ICP-MS). The data showed that the intracellular concentration of gold increased in a time-dependent manner in A549 cells, while a lower accumulation of Au-1 a@MSN(R) was found in L02 cells (Figure 2 b). For instance, after 8 hours incubation, the intracellular gold concentration in A549 cells was approximately 3.25 times higher than that in L02 cells. To further demonstrate the high selectivity of the nanosystem towards cancer cells, we used a co-culture model with A549 and L02 cells to examine the selective induction of apoptosis by Au-1 a@MSN(R) in cancer cells by conducting TUNEL–Hoechst 33342 co-staining assay experiments. This assay can detect DNA fragmentation in apoptotic cells, even before morphological changes. As shown in Figure 2 c, the control A549 cells did not show apoptotic characteristics. After treatment with Au-1 a@MSN(R) (1.0 μM), most A549 cells exhibited typical apoptotic features, including cell shrinkage, DNA fragmentation, and nuclear condensation, whereas these changes were not found in L02 cells. The apoptotic percentages of A549 cells in the co-culture population exposed to 0.5 and 1.0 μM Au-1 a@MSN(R) were 45 % and 54 %, respectively, which were significantly higher than those of L02 cells (1 % and 2 %, respectively). In contrast, 2.5 μM of Au-1 a (which exhibits a similar growth inhibition of

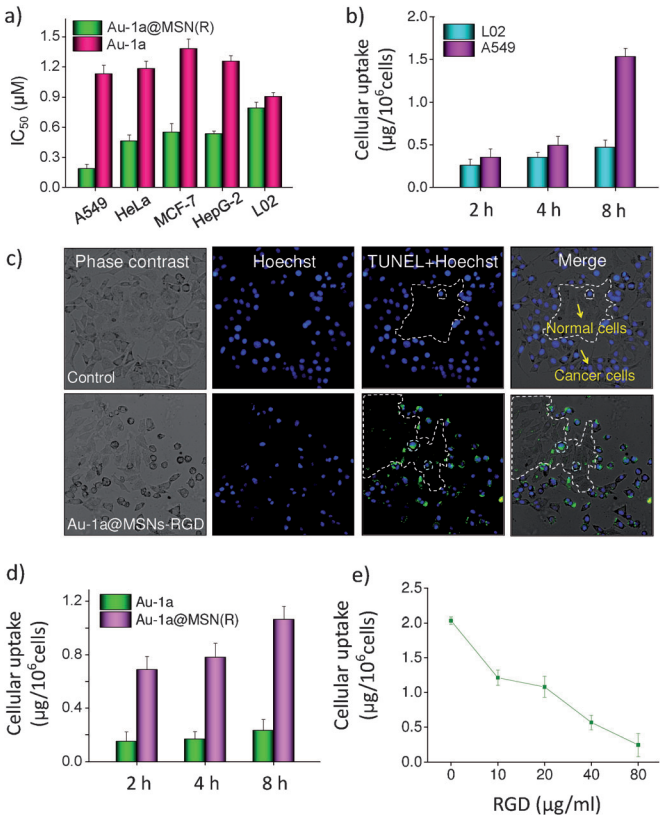

Figure 2. Selectivity and cellular uptake of Au-1a@MSN(R). a) Cytotoxic effects of Au-1a@MSN(R) and Au-1a on various human cancer and normal cell lines after 72 hours incubation. b) Quantitative analysis of cellular uptake of Au-1a@MSN(R) (2.0 μM) in L02 normal human liver cells and A549 lung carcinoma cell lines. c) Selective induction of apoptosis by Au-1a@MSN(R) (1.0 μM; 24 hours) in a A549/L02 co-culture cell model as determined by TUNEL-Hoechst 33342 co-staining microscopy (magnification, 200×). d) Quantitative analysis of cellular uptake in A549 cells after incubation with Au-1a and Au-1a@MSN(R) (each at 2.0 μM). e) Dose-dependent effects of RGD peptide on the cellular uptake of Au-1a@MSN(R). The cells were treated with RGD for 2 hours, and then exposed to Au-1a@MSN(R) (2.0 μM) for 12 hours.

A549 cells as demonstrated with 1.0 μM Au-1a@MSN(R)) induced 23% and 24% apoptosis in A549 and L02 cells, respectively (Figure S11). These results suggest that the nanosystem effectively improves the selectivity of Au-1a between cancer and normal cells.

Conjugation of RGD peptide to nanoparticles could help the RGD peptide to recognize and bind to integrin proteins which are overexpressed in cancer cell membranes, thereby enhancing the cellular uptake of nanoparticles in cancer cells.[8b] To examine the role of integrin, an RGD peptide competing assay was conducted. First, we examined the intracellular concentration of gold in A549 cells using ICP-MS after the cells were incubated with Au-1a (2.0 μM) and Au-1a@MSN(R) (2.0 μM) for different periods of time. As shown in Figure 2d, the intracellular concentration of gold in cells treated with Au-1a@MSN(R) increased significantly in a time-dependent manner, whereas it only slightly increased in cells exposed to Au-1a over a time period of 2–8 hours. These results indicate that encapsulation effectively enhances the cellular uptake of Au-1a in cancer cells. Moreover, the cellular internalization of Au-1a@MSN(R) was significantly decreased when the cells were pretreated with RGD peptides for 2 hours (Figure 2e). These results are consistent with the hypothesis that the high selectivity of the nanosystem incorporating the gold complex Au-1a could be traced to integrin-mediated endocytosis.

As A549 cells exhibited the highest sensitivity to Au-1a@MSN(R), this cell line was chosen for further investigation of the underlying mechanisms accounting for the anticancer activity. First, the results of flow cytometric analysis revealed that treatment of A549 cells with Au-1a@MSN(R) (0.25–1.0 μM) resulted in a marked dose-dependent increase in cell apoptosis as shown by extensive DNA fragmentation in the sub-G_1 phase. The apoptosis-inducing effect was even more pronounced compared with free Au-1a (2.5 μM; Figure S12). Caspase activation is a critical event in the initiation and execution of apoptosis in biological systems.[17] As shown in Figure S13, exposure of A549 cells to Au-1a@MSN(R) resulted in activation of caspase-3, caspase-8, caspase-9, and subsequent cleavage of PARP (poly(ADP-ribose)polymerase) in a dose-dependent manner. These results demonstrate that cancer-targeted MSN effectively enhances the apoptosis-inducing activity of Au-1a.

TrxR plays important roles in intracellular redox balance and regulation of apoptosis signaling. We have reported the inhibition of TrxR activity by anticancer gold complexes.[5d,18] As shown in Figure 3a, Au-1a@MSN(R) significantly inhibited the TrxR activity in a dose-dependent manner in A549 cells. For instance, TrxR activity of A549 cells decreased to about 16.8% of the control value after incubation with Au-1a@MSN(R) (1.0 μM). In contrast, Au-1a at 1.0 μM only inhibited the TrxR activity to 46.9%. The results of Western blot analysis also showed that Au-1a@MSN(R) effectively inhibited the expression level of TrxR and Trx in cancer cells (Figure 3b). Therefore, the decrease in expression of TrxR and Trx may contribute to the anticancer efficacy of Au-1a@MSN(R) and its inhibition of TrxR activity.

The intracellular Trx system could control the cell fate by regulating the intracellular redox balance through counteracting excess reactive oxygen species (ROS).[19] The inhibition of TrxR and Trx may disturb the balance of intracellular ROS generation in cancer cells. Therefore, we examined the ROS level in A549 cells exposed to Au-1a, Au-1a@MSN(R), and the MSN carrier alone by using the fluorescent dye dihydroethidium (DHE) as a probe. As shown in Figure 4a, treatment of the cells with Au-1a@MSN(R) resulted in a rapid and significant increase in intracellular ROS generation in a time- and dose-dependent manner, whereas an equal amount of the drug carrier MSN alone induced a much lower increase in ROS generation in A549 cells. In contrast, Au-1a (at up to 40 μM concentration) did not trigger the overproduction of reactive oxygen species in this cell line under similar conditions. Thus, the induction of ROS overproduction may play a crucial role in the enhanced anticancer efficacy of Au-1a incorporated within the MSN nanosystem.

Excess intracellular ROS could activate diverse signaling pathways to trigger cell apoptosis.[20] As depicted in Fig-

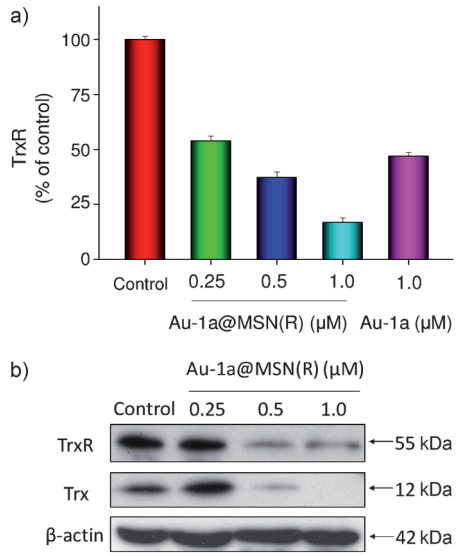

Figure 3. a) Inhibition of TrxR activity by Au-1 a@MSN(R) in A549 cells for 24 hours. b) Western blot analysis of expression levels of TrxR and Trx in A549 cells treated with Au-1 a@MSN(R) for 24 hours.

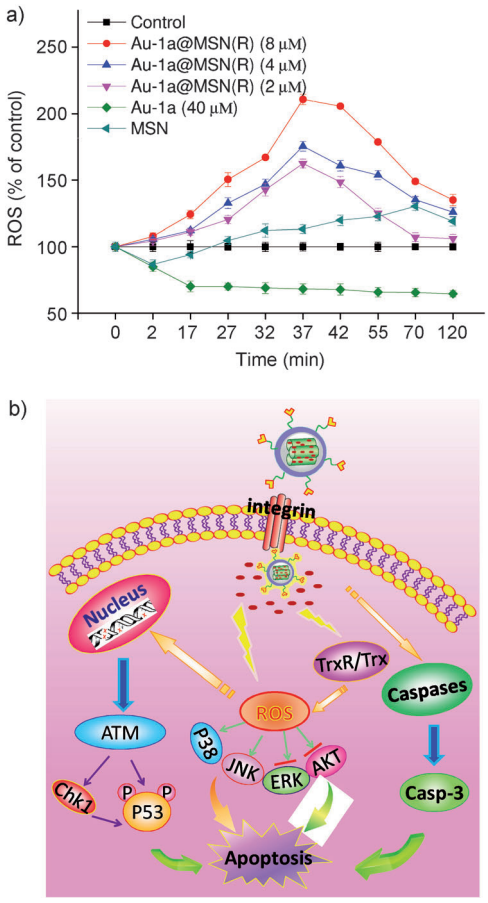

Figure 4. Activation of apoptotic signaling pathways in cancer cells by Au-1 a@MSN(R). a) Plot showing the overproduction of ROS against time in A549 cells exposed to Au-1 a@MSN(R), Au-1 a, and MSN (1.5 mg mL^{-1}). b) Proposed signaling pathways of apoptosis induced by Au-1 a@MSN(R).

ure S14, the phosphorylation of pro-apoptotic kinases p38 and JNK increased in a dose-dependent manner. In contrast, the phosphorylation of the two anti-apoptotic kinases ERK and AKT were effectively suppressed by Au-1 a@MSN(R). Moreover, cellular ROS accumulation induced by Au-1 a@MSN(R) resulted in DNA damage as revealed by increased expression of various protein markers. As shown in Figure S15, treatment of cells with Au-1 a@MSN(R) resulted in elevation of phosphorylated p53 at the serine 15 site. The protein levels of phospho-ATM, phospho-Chk1, phospho-BRCA1, and a DNA damage marker Ser139-Histone $H_2A.X$ were also upregulated in response to cell treatment with Au-1 a@MSN(R). Collectively, Au-1 a@MSN(R) could inhibit the TrxR system, which may subsequently trigger ROS-mediated apoptosis signaling in cancer cells (Figure 4 b).

In summary, we have synthesized a cancer-targeted mesoporous silica nanoparticle system to overcome the high toxicity of anticancer gold complexes and to enhance their anticancer efficacy. The RGD peptide surface decoration effectively enhances the cellular uptake of the drugs, and increases the recognition between cancer and normal cells. The efficacy and safety index of Au-1 a@MSN(R) is greater than that of the free Au-1 a complex. Encapsulation amplified the inhibitory effects of Au-1 a on the enzyme thioredoxin reductase (TrxR). This study highlights the usefulness of cancer-targeted nanoparticles for delivery of anticancer gold(III) porphyrin molecules to achieve enhanced anticancer efficacy with fewer side effects.

Received: July 12, 2014
Revised: August 13, 2014
Published online: September 12, 2014

Keywords: drug delivery · gold · mesoporous materials · porphyrins · silica nanoparticles

[1] a) M. Markman, *Expert Opin. Drug Saf.* **2003**, *2*, 597–607; b) P. C. Bruijnincx, P. J. Sadler, *Curr. Opin. Chem. Biol.* **2008**, *12*, 197–206.

[2] a) C. X. Zhang, S. J. Lippard, *Curr. Opin. Chem. Biol.* **2003**, *7*, 481–489; b) Y. Wang, Q. Y. He, R. W. Sun, C.-M. Che, J. F. Chiu, *Cancer Res.* **2005**, *65*, 11553–11564; c) D. Saggioro, M. P. Rigobello, L. Paloschi, A. Folda, S. A. Moggach, S. Parsons, L. Ronconi, D. Fregona, A. Bindoli, *Chem. Biol.* **2007**, *14*, 1128–1139; d) X. Wang, Z. Guo, *Dalton Trans.* **2008**, 1521–1532; e) K. H. Chow, R. W.-Y. Sun, J. B. Lam, C. K. Li, A. Xu, D. L. Ma, R. Abagyan, Y. Wang, C.-M. Che, *Cancer Res.* **2010**, *70*, 329–337; f) R. W.-Y. Sun, C. K. Li, D.-L. Ma, J. J. Yan, C.-N. Lok, C. H. Leung, N. Zhu, C.-M. Che, *Chem. Eur. J.* **2010**, *16*, 3097–3113; g) C.-M. Che, R. W.-Y. Sun, *Chem. Commun.* **2011**, *47*, 9554–9560.

[3] a) L. Messori, F. Abbate, G. Marcon, P. Orioli, M. Fontani, E. Mini, T. Mazzei, S. Carotti, T. O'Connell, P. Zanello, *J. Med. Chem.* **2000**, *43*, 3541–3548; b) E. Gao, C. Liu, M. Zhu, H. Lin, Q. Wu, L. Liu, *Anti-Cancer Agents Med. Chem.* **2009**, *9*, 356–368; c) F. Tisato, C. Marzano, M. Porchia, M. Pellei, C. Santini, *Med. Res. Rev.* **2010**, *30*, 708–749; d) G. N. Kaluderovic, R. Paschke, *Curr. Med. Chem.* **2011**, *18*, 4738–4752.

[4] a) I. Ott, X. Qian, Y. Xu, D. H. Vlecken, I. J. Marques, D. Kubutat, J. Will, W. S. Sheldrick, P. Jesse, A. Prokop, C. P. Bagowski, *J. Med. Chem.* **2009**, *52*, 763–770; b) R. Rubbiani, I.

Kitanovic, H. Alborzinia, S. Can, A. Kitanovic, L. A. Onambele, M. Stefanopoulou, Y. Geldmacher, W. S. Sheldrick, G. Wolber, A. Prokop, S. Wolfl, I. Ott, *J. Med. Chem.* **2010**, *53*, 8608 – 8618; c) C. Marzano, L. Ronconi, F. Chiara, M. C. Giron, I. Faustinelli, P. Cristofori, A. Trevisan, D. Fregona, *Int. J. Cancer* **2011**, *129*, 487 – 496; d) E. Jortzik, M. Farhadi, R. Ahmadi, K. Toth, J. Lohr, B. M. Helmke, S. Kehr, A. Unterberg, I. Ott, R. Gust, V. Deborde, E. Davioud-Charvet, R. Reau, K. Becker, C. Herold-Mende, *Biochim. Biophys. Acta* **2014**, *1844*, 1415 – 1426.

[5] a) S. Urig, K. Fritz-Wolf, R. Reau, C. Herold-Mende, K. Toth, E. Davioud-Charvet, K. Becker, *Angew. Chem. Int. Ed.* **2006**, *45*, 1881 – 1886; *Angew. Chem.* **2006**, *118*, 1915 – 1920; b) J. L. Hickey, R. A. Ruhayel, P. J. Barnard, M. V. Baker, S. J. Berners-Price, A. Filipovska, *J. Am. Chem. Soc.* **2008**, *130*, 12570 – 12571; c) E. Meggers, *Chem. Commun.* **2009**, 1001 – 1010; d) T. Zou, C. T. Lum, C.-N. Lok, W.-P. To, K.-H. Low, C.-M. Che, *Angew. Chem. Int. Ed.* **2014**, *53*, 5810 – 5814; *Angew. Chem.* **2014**, *126*, 5920 – 5924; e) G. Gasser, I. Ott, N. Metzler-Nolte, *J. Med. Chem.* **2011**, *54*, 3 – 25.

[6] a) C.-M. Che, R. W.-Y. Sun, W.-Y. Yu, C.-B. Ko, N. Zhu, H. Sun, *Chem. Commun.* **2003**, 1718 – 1719; b) Y. Wang, Q. Y. He, C.-M. Che, J. F. Chiu, *Proteomics* **2006**, *6*, 131 – 142; c) Y. Wang, Q. Y. He, R. W. Sun, C.-M. Che, J. F. Chiu, *Eur. J. Pharmacol.* **2007**, *554*, 113 – 122; d) Y. Wang, Q. Y. He, C.-M. Che, S. W. Tsao, R. W. Sun, J. F. Chiu, *Biochem. Pharmacol.* **2008**, *75*, 1282 – 1291; e) W. Li, Y. Xie, R. W. Sun, Q. Liu, J. Young, W. Y. Yu, C.-M. Che, P. K. Tam, Y. Ren, *Br. J. Cancer* **2009**, *101*, 342 – 349.

[7] C.-N. Lok, T. Zou, J.-J. Zhang, I. W. Lin, C.-M. Che, *Adv. Mater.* **2014**, *26*, 5550 – 5557.

[8] a) V. J. C. Y. Mohanraj, *Trop. J. Pharm. Res.* **2006**, *5*, 561 – 574; b) D. Peer, J. M. Karp, S. Hong, O. C. Farokhzad, R. Margalit, R. Langer, *Nat. Nanotechnol.* **2007**, *2*, 751 – 760; c) J. J. Yan, R. W.-Y. Sun, P. Wu, M. C. M. Lin, A. S. C. Chan, C.-M. Che, *Dalton Trans.* **2010**, *39*, 7700 – 7705; d) N. Graf, S. J. Lippard, *Adv. Drug Delivery Rev.* **2012**, *64*, 993 – 1004; e) J. S. Butler, P. J. Sadler, *Curr. Opin. Chem. Biol.* **2013**, *17*, 175 – 188; f) H. S. Oberoi, N. V. Nukolova, A. V. Kabanov, T. K. Bronich, *Adv. Drug Delivery Rev.* **2013**, *65*, 1667 – 1685; g) J. Yao, M. Yang, Y. Duan, *Chem. Rev.* **2014**, *114*, 6130 – 6178; h) Y. Wang, M. S. Shim, N. S. Levinson, H.-W. Sung, Y. Xia, *Adv. Funct. Mater.* **2014**, *24*, 4206 – 4220.

[9] a) W. Gao, R. Langer, O. C. Farokhzad, *Angew. Chem. Int. Ed.* **2010**, *49*, 6567 – 6571; *Angew. Chem.* **2010**, *122*, 6717 – 6721; b) S. Aryal, C. M. Hu, L. Zhang, *ACS Nano* **2010**, *4*, 251 – 258; c) S. Dufort, L. Sancey, J. L. Coll, *Adv. Drug Delivery Rev.* **2012**, *64*, 179 – 189; d) Y. Wu, W. Chen, F. Meng, Z. Wang, R. Cheng, C. Deng, H. Liu, Z. Zhong, *J. Controlled Release* **2012**, *164*, 338 – 345; e) S. Huo, H. Ma, K. Huang, J. Liu, T. Wei, S. Jin, J. Zhang, S. He, X. J. Liang, *Cancer Res.* **2013**, *73*, 319 – 330; f) S. H. Medina, M. V. Chevliakov, G. Tiruchinapally, Y. Y. Durmaz, S. P. Kuruvilla, M. E. Elsayed, *Biomaterials* **2013**, *34*, 4655 – 4666.

[10] a) M. Vallet-Regi, A. Rámila, R. P. del Real, J. Pérez-Pariente, *Chem. Mater.* **2001**, *13*, 308 – 311; b) S. Hudson, J. Cooney, E. Magner, *Angew. Chem. Int. Ed.* **2008**, *47*, 8582 – 8594; *Angew. Chem.* **2008**, *120*, 8710 – 8723; c) J. Shi, A. R. Votruba, O. C. Farokhzad, R. Langer, *Nano. Lett.* **2010**, *10*, 3223 – 3230; d) V. Lebret, L. Raehm, J. O. Durand, M. Smaihi, M. H. Werts, M. Blanchard-Desce, D. Methy-Gonnod, C. Dubernet, *J. Biomed. Nanotechnol.* **2010**, *6*, 176 – 180; e) J. L. Vivero-Escoto, I. I. Slowing, B. G. Trewyn, V. S. Lin, *Small* **2010**, *6*, 1952 – 1967; f) R. Hao, R. Xing, Z. Xu, Y. Hou, S. Gao, S. Sun, *Adv. Mater.* **2010**, *22*, 2729 – 2742; g) Z. Li, J. C. Barnes, A. Bosoy, J. F. Stoddart, J. I. Zink, *Chem. Soc. Rev.* **2012**, *41*, 2590 – 2605; h) P. Yang, S. Gai, J. Lin, *Chem. Soc. Rev.* **2012**, *41*, 3679 – 3698.

[11] Y. Fang, G. Zheng, J. Yang, H. Tang, Y. Zhang, B. Kong, Y. Lv, C. Xu, A. M. Asiri, J. Zi, F. Zhang, D. Zhao, *Angew. Chem. Int. Ed.* **2014**, *53*, 5366 – 5370; *Angew. Chem.* **2014**, *126*, 5470 – 5474.

[12] Y.-S. Lin, C. L. Haynes, *J. Am. Chem. Soc.* **2010**, *132*, 4834 – 4842.

[13] a) P. D. Thornton, A. Heise, *J. Am. Chem. Soc.* **2010**, *132*, 2024 – 2028; b) N. Singh, A. Karambelkar, L. Gu, K. Lin, J. S. Miller, C. S. Chen, M. J. Sailor, S. N. Bhatia, *J. Am. Chem. Soc.* **2011**, *133*, 19582 – 19585; c) C. E. Ashley, E. C. Carnes, G. K. Phillips, D. Padilla, P. N. Durfee, P. A. Brown, T. N. Hanna, J. Liu, B. Phillips, M. B. Carter, N. J. Carroll, X. Jiang, D. R. Dunphy, C. L. Willman, D. N. Petsev, D. G. Evans, A. N. Parikh, B. Chackerian, W. Wharton, D. S. Peabody, C. J. Brinker, *Nat. Mater.* **2011**, *10*, 389 – 397; d) F. Muhammad, M. Guo, W. Qi, F. Sun, A. Wang, Y. Guo, G. Zhu, *J. Am. Chem. Soc.* **2011**, *133*, 8778 – 8781; e) Y. Zhang, M. Wang, Y.-g. Zheng, H. Tan, B. Y.-w. Hsu, Z.-c. Yang, S. Y. Wong, A. Y.-c. Chang, M. Choolani, X. Li, J. Wang, *Chem. Mater.* **2013**, *25*, 2976 – 2985.

[14] a) K. Obara, M. Ishihara, Y. Ozeki, T. Ishizuka, T. Hayashi, S. Nakamura, Y. Saito, H. Yura, T. Matsui, H. Hattori, B. Takase, M. Ishihara, M. Kikuchi, T. Maehara, *J. Controlled Release* **2005**, *110*, 79 – 89; b) M. C. Gutiérrez, Z. Y. García-Carvajal, M. Jobbágy, F. Rubio, L. Yuste, F. Rojo, M. L. Ferrer, F. del Monte, *Adv. Funct. Mater.* **2007**, *17*, 3505 – 3513; c) W. Wei, L. Yuan, G. Hu, L.-Y. Wang, J. Wu, X. Hu, Z.-G. Su, G.-H. Ma, *Adv. Mater.* **2008**, *20*, 2292 – 2296; d) F. Chen, Y. Zhu, *Microporous Mesoporous Mater.* **2012**, *150*, 83 – 89.

[15] L. He, Y. Huang, H. Zhu, G. Pang, W. Zheng, Y.-S. Wong, T. Chen, *Adv. Funct. Mater.* **2014**, *24*, 2737 – 2915.

[16] C. T. Lum, R. W.-Y. Sun, T. Zou, C.-M. Che, *Chem. Sci.* **2014**, *5*, 1579 – 1584.

[17] I. Budihardjo, H. Oliver, M. Lutter, X. Luo, X. Wang, *Annu. Rev. Cell Dev. Biol.* **1999**, *15*, 269 – 290.

[18] a) K. Yan, C. N. Lok, K. Bierla, C.-M. Che, *Chem. Commun.* **2010**, *46*, 7691 – 7693; b) R. W.-Y. Sun, C.-N. Lok, T. T.-H. Fong, C. K.-L. Li, Z. F. Yang, T. Zou, A. F.-M. Siu, C.-M. Che, *Chem. Sci.* **2013**, *4*, 1979 – 1988.

[19] C. Fan, W. Zheng, X. Fu, X. Li, Y. S. Wong, T. Chen, *Cell Death Differ.* **2014**, 5, e1191.

[20] T. Chen, Y. S. Wong, *Cell. Mol. Life Sci.* **2008**, *65*, 2763 – 2775.